Colour Vision Properties of Surface Colours based on complementary Optimal Colours

Klaus Richter

Berlin University of Technology (TUB), GERMANY

*klaus.richter@mac.com

ABSTRACT

Nearly all surface colours are located within a colour solid which is defined by complementary optimal colours and white and black. Special optimal colours with wavelength limits of a "colour half" are called *Ostwald* colours. One *Ostwald* "colour half", for example with the complementary wavelength limits 470 and 570 nm and the other "colour half" with the wavelength limits 570 and 470 nm, mix two white and are called *antichromatic* colours. The chromatic value is defined by the product of the chromaticty difference of cone excitations and the tristimulus value Y. For example for Yellow the tristimulus value Y is by a factor 8 larger compared to Blue. This is opposite for the chromaticity difference. Therefore the chromatic value is approximately constant for all *Ostwald* colours. The cone sensitivities are calculated from the CIE spectral tristimulus values. Three parable functions of the same shape with peak wavelengths 430, 540 and 570 nm are used in a model. The model can describe the four elementary hues Blue B_e, Green G_e, Yellow Y_e and Red R_e.

KEYWORDS: surface colours, optimal colours, elementary (unique) hues

INTRODUCTION

There are different colour vision properties for related surface colours and unrelated colours in lightimg technology. This paper studies special surface colours which are complementary optimal colours of a colour half and which are called *Ostwald* colours. The spectral reflection has the value one for a colour half and zero for the other half. The spectral wavelength limits of these colour halves are located on a line in the CIE (x, y) chromaticity diagram through the chromaticity (x_n, y_n) of or near CIE illuminant D50 which is a *natural* achromatic colour compared to the bluish CIE illuminant 65 and the yellowish CIE illuminant A. For D50 the *Ostwald* colours are placed approximately on a circle in a chromatic value diagram (see [1], Table 3 and Fig. 58 for D65, the larger yellow blue extension reduces for D50, see Fig. 6c in the following).

In the following the cone sensitivities, the cone excitations, and the tristimulus value excitations are modeled by parables as function of wavelength. Fig. 5c is based on this model and allows to understand the existence of elementary colours and their spectral distribution. Fig. 6c shows the chromatic values of the *Ostwald* colours. The chromatic value A_1 is based on the colour confusion lines of tritanopic observers.

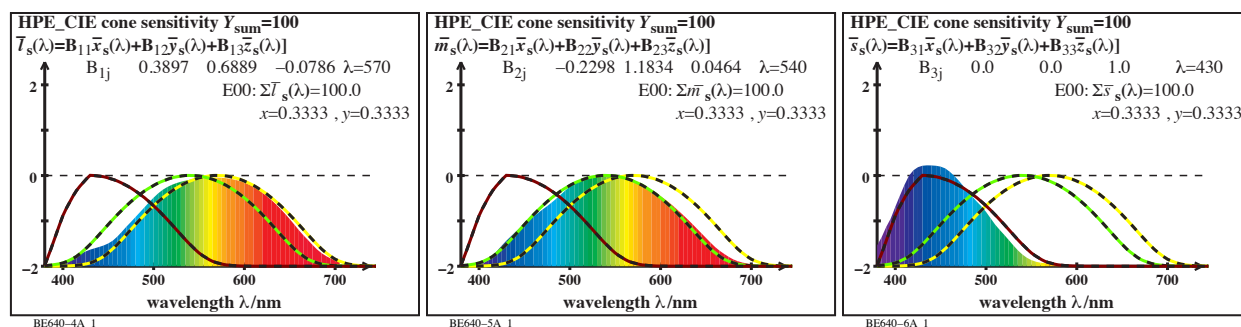## THEORY AND EXPERIMENTAL RESULTS

Fig 1(a, b, c): HPE-cone sensitivities and parable functions with maximum values at 570, 540, 430nm

Fig 1 shows the cone sensitivities LMS which are calculated by the *Hunt-Pointer-Estevez* (HPE) transformation from the CIE spectral tristimulus values. The transformation equations are given in Fig. 1. The data are still used in a new CIE Technical Report [2]. Many books on colorimetry propose similar peak values, for example the data 564, 534, and 420 nm of *Oleari* in [3, page 82]. The colour-black dashed lines model the three cone sensitivities $l(\lambda)$, $m(\lambda)$, and $s(\lambda)$ by three parable functions in log units. In the short wavelength range below 530 nm the $s(\lambda)$ sensitivity is reduced by the eye media in the fovea, see [3, Fig. 5.4].
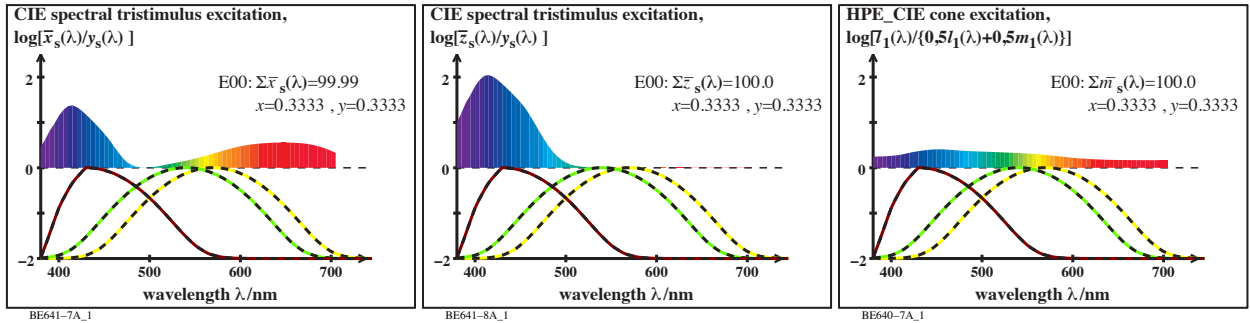

Fig. 2(a, b, c): CIE spectral tristimulus value and cone excitations

Fig. 2 shows excitations of the CIE tristimulus values X and Z and the L cone. The excitation is the ratio of the value and the tristimulus value Y. Similar the ratio of the tristimulus values X/Y, Z/Y, and L/Y can be used. The Y value is a linear transformation of the cone values L and M. Instead of the tristimulus values the spectral values are used in Fig. 2 and the following. Fig. 2c may not be useful for applications.
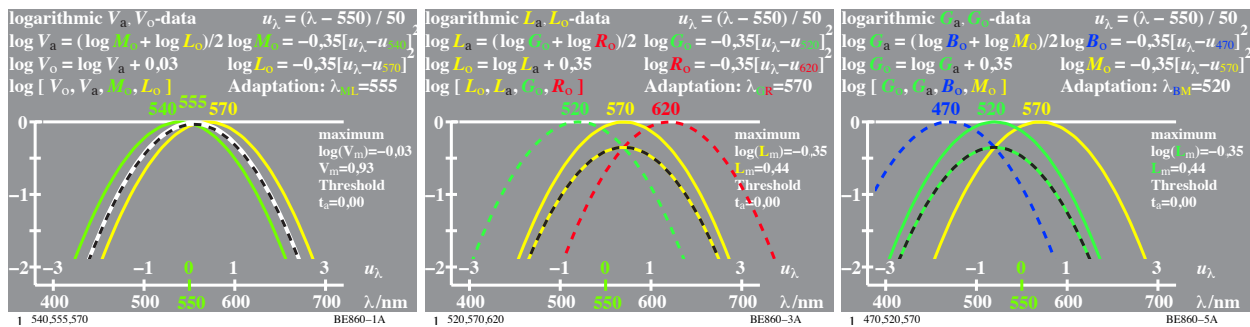

Fig. 3(a, b, c): Logarithmic sum and differences of the spectral cone sensitivities

Fig. 3 shows example calculations of the sum and differences of the spectral cone sensitivities L and M. The peak values of L (570 nm, yellow curve) and M (540 nm, green curve) have a difference of 30 nm. The yellow and green colour is used here to indicate that the peak value is in the yellow or green spectral range. The logarithmic sum and for example a linear sum differs by only 1% near 400nm and 700nm [3, Fig. 4-36]. The threshold value is 2% compared to the maximum value for surface colours, see [3, Fig. 6.17]. Therefore a decision of a linear or logarithmic sum is not possible in the case of surface colours. There is a long expert discussion about the ratio of the weighting factors. The ratio 1:1 is used in Fig. 2c and the ratio 1:2 is used in the HPE transformation. Recent studies show that there are large individual variations in the relative numbers of cone types and their distribution in the retina [3, section 5.4.6].

A logarithmic calculation in Fig. 3 allows to calculate the same shape for these experimental variations in cone distributions. Equations (1) to (5) show examples used in the plots of Fig. 3 and the following.

$$\log V_a = 0.5 \,[\log M_o + \log L_o] \tag{1}$$
or
$$V_a = (M_o \times L_o)^{0,5} \tag{2}$$
or
$$\log M_o = 2 \log V_a - \log L_o \tag{3}$$
with
$$\log V_o = \log V_a + 0.03 \tag{4}$$

The cone excitation is the logarithmic linear ratio or the logarithmic difference

$$\log (M_o / V_a) = \log M_o - \log V_a \tag{5}$$

If the peak values are normalized to one the index (o) is used. The sum and differences produce peak values below one and in this paper then the index (a) is used. The symbols V_a (white-black curve) and V_o (white curve), see Fig. 3a are proportional to the luminous tristimulus value Y. $V_a(\lambda)$ is smaller compared to $V_o(\lambda)$ by the factor 0,97 in logarithmic units and 0,93 in linear units. See also more values in Fig. 3b and 3c.

In Fig 3a the functions $V_a(\lambda)$ and $V_o(\lambda)$ are calculated according to equation (1). Similar in Fig. 3b the $L_a(\lambda)$ and $L_o(\lambda)$ functions are calculated from *calculated* sensitivities $R_o(\lambda)$ and $G_o(\lambda)$. All *calculated* sensitivities are shown by *dashed* curves. Fig. 3b uses the red and green colours according to the location in the spectral range. Fig. 3c is similar with peak values 570, 520, and 470 nm. These are the peak values of the spectral elementary colours, for example the elementary (e) green G_e as neither yellowish nor bluish.
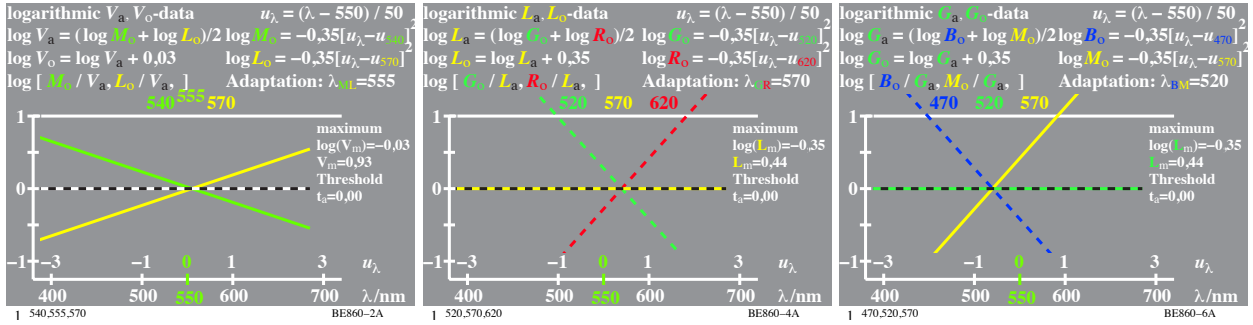

Fig. 4(a, b, c): Cone excitation as logarithmic ratio of the spectral or *calculated* cone sensitivities

Fig. 4 shows the logarithmic ratio of the real or *calculated* cone sensitivities in Fig. 3a to 3b as function of wavelength according to equation (5). The slope increases with the difference of the peak values.
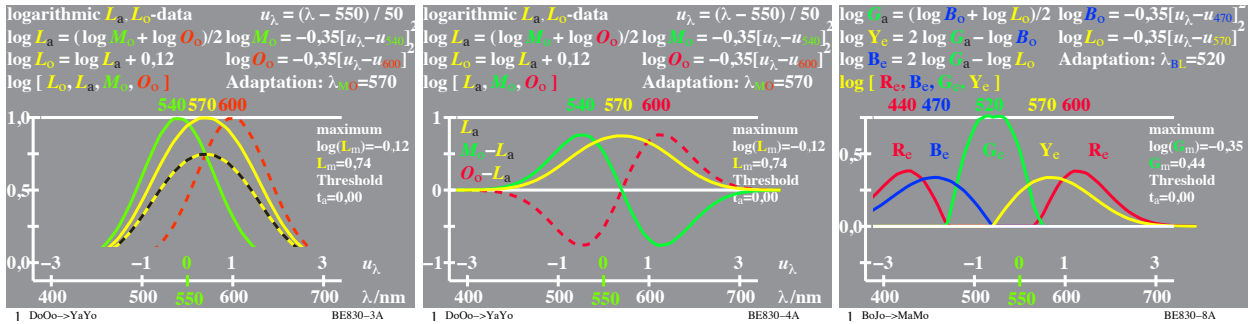

Fig. 5(a, b, c): Sensitivities M (540nm), L (570nm), and O (600nm) on a linear ordinate.

Fig 5a shows a linear ordinate scale for three sensitivities M_o, L_o, and O_o. L_a is calculated by the logarithmic sum of M_o and O_o. Fig. 5b shows the linear differences of Fig. 5a. For the sensitivity difference $O_o(\lambda) - L_a(\lambda)$ a dashed curve in red is used because the sensitivity $O_o(\lambda)$ is a *calculated* sensitivity. Together with similar functions in the blue part around 470 nm (of smaller values?) the hue appearance in the spectral range according to the elementary (e) colours B_e, G_e, Y_e, and R_e can be described.
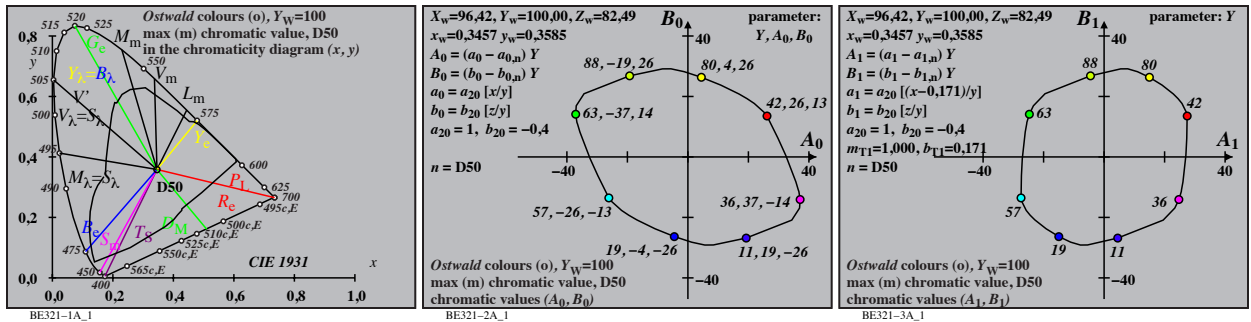

Fig 6(a, b, c): Peak sensitivities L_m, M_m, S_m , confusion lines of P_L, D_M, T_S observers, and elementary hues.

Fig. 6a shows the location of the peak sensitivities L_m, M_m, S_m, the confusion lines of P_L, D_M, T_S observers, the elementary hues B_e, G_e, Y_e, and R_e and all *Ostwald* colours in the CIE chromaticity diagram (x, y). Fig. 6b and 6c show the chromatic value of the *Ostwald* colours under an illumination which appears *natural* white. The CIE standard illuminant D50 is near the *natural* white. The CIE daylight D65 (CCT 6500K) appears bluish and a tungsten light (CCT 3000K) is yellowish. An illumination with a linear change of the CIE illumination $E(\lambda)$ of equal energy as function of λ appears similar to D50. The spectral distribution is $P(\lambda) = \lambda/560\text{nm } E(\lambda)$, and is called P00 in this paper. With the linear equations given in Fig. 6b and 6c the antichromatic *Ostwald* colours have antichromatic colour values and are located approximately on a circle. The chromaticities (x, y) are shown in Fig. 6a. The CIE tristimulus values differ by a factor 8 (between 88 and 11, see parameter Y in Fig. 6b or 6c. Therefore the tristimulus value excitation difference $a-a_n=x/y - x_n/y_n$ and similar for $b-b_n$ is by a factor 8 smaller for yellow Y_e compared to blue B_e.
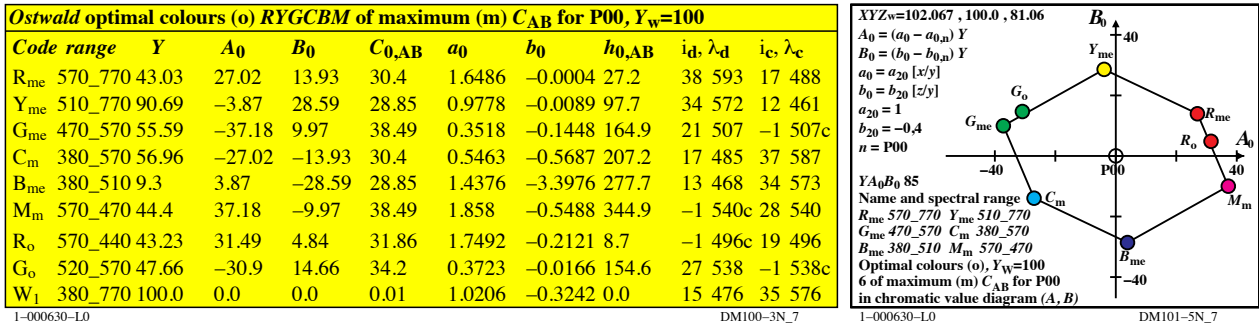
Ostwald optimal colours (o) RYGCBM of maximum (m) C_{AB} for P00, Y_W=100

Code range		Y	A_0	B_0	$C_{0,AB}$	a_0	b_0	$h_{0,AB}$	i_d, λ_d	i_c, λ_c
R_{me}	570_770	43.03	27.02	13.93	30.4	1.6486	−0.0004	27.2	38 593	17 488
Y_{me}	510_770	90.69	−3.87	28.59	28.85	0.9778	−0.0089	97.7	34 572	12 461
G_{me}	470_570	55.59	−37.18	9.97	38.49	0.3518	−0.1448	164.9	21 507	−1 507c
C_m	380_570	56.96	−27.02	−13.93	30.4	0.5463	−0.5687	207.2	17 485	37 587
B_{me}	380_510	9.3	3.87	−28.59	28.85	1.4376	−3.3976	277.7	13 468	34 573
M_m	570_470	44.4	37.18	−9.97	38.49	1.858	−0.5488	344.9	−1 540c	28 540
R_o	570_440	43.23	31.49	4.84	31.86	1.7492	−0.2121	8.7	−1 496c	19 496
G_o	520_570	47.66	−30.9	14.66	34.2	0.3723	−0.0166	154.6	27 538	−1 538c
W_1	380_770	100.0	0.0	0.0	0.01	1.0206	−0.3242	0.0	15 476	35 576

1–000630–L0   DM100–3N_7

$XYZ_w=102.067 , 100.0 , 81.06$
$A_0 = (a_0 − a_{0,n}) Y$
$B_0 = (b_0 − b_{0,n}) Y$
$a_0 = a_{20} [x/y]$
$b_0 = b_{20} [z/y]$
$a_{20} = 1$
$b_{20} = −0,4$
n = P00

YA_0B_0 85
Name and spectral range
R_{me} 570_770 Y_{me} 510_770
G_{me} 470_570 C_m 380_570
B_{me} 380_510 M_m 570_470
Optimal colours (o), Y_W=100
6 of maximum (m) C_{AB} for P00
in chromatic value diagram (A, B)

1–000630–L0   DM101–5N_7

Fig. 7(a, b): Chromatic values A_0, B_0, $C_{0,AB}$ and chromaticities (a, b) of *Ostwald* optimal colours

Fig. 7a shows the chromatic values A_0, B_0, and the chromaticities (a_0, b_0) of the *Ostwald* optimal colours. The chromaticity difference of any colour compared to the achromatic colour W_1 in Fig 7a is by a factor 8 different. If the difference is small the Y values is high and vice versa. In Fig. 1a the chromatic value $C_{0,AB}$ is approximately independent of hue and of the Y value for the antichromatic *Ostwald* optimal colours.

RESULTS AND DISCUSSION

The confusion lines T_S and P_L of the Tritanope (T) and Protanope (P) observers with missing L and S cones connect the achromatic and the chromaticity of 400 nm and 700 nm in Fig. 6a. The T_S line defines a basic chromatic value system (A_1, B_1), see Fig. 6c, to produce equal chromatic values for the *Ostwald* colours. In Fig. 6b the system (A_0, B_0) produces a slightly less performance. However, (A_0, B_0) matches the property of CIELAB that elementary yellow and blue is located on the vertical axis and both red and green are shifted about 30 degree upwards compared to the horizontal axis. Therefore, for the description of the hue angles the *linear* chromatic value diagram (A_o, B_o) is similar to the *cube root* chroma diagram (a^*, b^*) of CIELAB because of similar hue angles for the elementary colours [5]. An application example is given in CIE R1-57 [6] which uses the *Ostwald* colours to describe the border between blackish and luminous surface colours.

CONCLUSION AND FUTURE DEVELOPMENT

All *Ostwald* colours have approximately the same chromatic value $C_{0,AB}$, see Fig. 7a. For the *Ostwald* colours this is surprising because the tristimulus values Y and the tristimulus value excitations, for example $x/y = X/Y$ vary by a factor 8. The equal chromatic values of the *Ostwald* colours in Fig. 6c are a basis for a colorimetric description of the experimental results of *Holtsmark* and *Valberg* [7]. The experimental equal colour threshold for all antichromatic optimal colours needs the equal chromatic values. A following paper will develop an improved colour metric for surface colours and will use cone and tristimulus value excitations.

ACKNOWLEDGEMENT AND REMARKS

REFERENCES

[1] Richter, Klaus, 2016, Colour and Colour Vision and Elementary Colours in Colour Information Technology, 85 pages (A5), see http://farbe.li.tu-berlin.de/color. This paper includes printed achromatic and chromatic test charts with elementary colours according to ISO/IEC 15775, ISO/IEC TR 24705, and ISO/DIS 9241-306:2017, Annex D, see http:/standards.iso.org/iso/9241/306/ed-2/index.html

[2] CIE 224:2017. Colour Fidelity Index for accurate scientific use.

[3] Oleari, Claudio, 2016, Standard Colorimetry, Definitions, Algorithms and Software, Wiley

[4] Richter, Klaus, 1996, Computergrafik und Farbmetrik, Farbsysteme, http://farbe.li.tu-berlin.de/buche.html

[5] Thorstein Seim, 2009, Reportership Report CIE R1-47, Hue angles of elementary colours (35 pages), see http://files.cie.co.at/526.pdf

[6] Thorstein Seim, 2013, Reportership Report CIE R1-57, Border between Blackish and Luminous Colours, (23 pages), see http://files.cie.co.at/716_CIE%20R1-57%20Report%20Jul-13%20v.2.pdf

[7] Holtsmark, T. and Valberg, A. (1969), Colour discrimination and hue, Nature, Volume 224, 366-367.